

Multi-layer Kernel Ridge Regression for One-class Classification

Chandan Gautam^{a,*}, Aruna Tiwari^a, Sundaram Suresh^b, Alexandros Iosifidis^c

^aIndian Institute of Technology Indore, Indore, Simrol, India

^bSchool of Electrical and Electronic Engineering, Nanyang Technological University Singapore

^cAarhus University, Denmark

Abstract

In this paper, a multi-layer architecture (in a hierarchical fashion) by stacking various Kernel Ridge Regression (*KRR*) based Auto-Encoder for one-class classification is proposed and is referred as MKOC. MKOC has many layers of Auto-Encoders to project the input features into new feature space and the last layer is regression based one class classifier. The Auto-Encoders use an unsupervised approach of learning and the final layer uses semi-supervised (trained by only positive samples) approach of learning. The proposed MKOC is experimentally evaluated on 15 publicly available benchmark datasets. Experimental results verify the effectiveness of the proposed approach over 11 existing state-of-the-art kernel-based one-class classifiers. Friedman test is also performed to verify the statistical significance of the claim of the superiority of the proposed one-class classifiers over the existing state-of-the-art methods.

Keywords: One-class Classification, Outlier Detection, Kernel Ridge Regression, Kernel Learning, Multi-layer.

1. Introduction

One-class Classification (OCC) has been widely used for outlier, novelty, fault, and intrusion detection [1, 2, 3, 4] by researchers from different disciplines. In OCC problems, samples of the class of interest (i.e., positive samples) are available while negative samples are very rare or costly to collect [5, 6, 7, 8, 9], thus making the application of multi-class models problematic. Various one-class classifiers [1, 2] have been proposed based on the regression model, the clustering model etc. One-class classification methods available in the literature can be divided into two broad categories viz., non-kernel-based and kernel-based methods. Various non-kernel-based one-class classifiers are principal component analysis based data descriptor¹ [5], angle-based outlier factor data description [10], K-means data

*Corresponding author

Email addresses: chandangautam31@gmail.com (Chandan Gautam), artiwari@iiti.ac.in (Aruna Tiwari), ssundaram@ntu.edu.sg (Sundaram Suresh), alexandros.iosifidis@eng.au.dk (Alexandros Iosifidis)

¹One-class classifiers are also known as data descriptors due to their capability to describe the distribution of data and the boundaries of the class of interest

description [5], self-organizing map data description [5], Auto-Encoder data descriptor [11] etc. Whereas, the kernel-based one-class classifier approaches are support vector data description [12], one-class support vector machine[13], kernel principal component analysis based data description[14] etc. However, kernel-based methods have been shown to outperform non-kernel-based methods in the literature [1, 5]. Despite this fact, these kernel-based methods involve the solution of a quadratic optimization problem, which is computationally expensive. Apart of these kernel-based methods, *KRR*-based models [15] optimize the problem rapidly in a non-iterative way by solving a linear systems. Therefore, *KRR*-based models [15, 16, 17, 18, 19] have received quite attention by researchers for solving various types of problems viz., regression, binary, multi-class etc.

In recent years, various *KRR*-based one-class classifiers have been developed and exhibited better performance compared to various state-of-the-art one-class classifiers. Overall, the *KRR*-based one-class classifiers can be divided into two types, namely, (i) without Graph-Embedding (ii) with Graph-Embedding. For ‘without Graph-Embedding’, two types of architectures have been explored for OCC. One is *KRR*-based single output node architecture [20], and other is *KRR*-based Auto-Encoder architecture [21]. For ‘with Graph-Embedding’, Iosifidis et al.[22] presented local and global structure. Different types of Laplacian Graphs are employed for local (i.e., Local Linear Embedding, Laplacian Eigenmaps etc.) and global (linear discriminant analysis and clustering-based discriminant analysis etc.) Graph-embedding. Later, global variance-based Graph-Embedding has been extended in order to exploit class variance and sub-class variance information for face verification task by Mygdalis et al.[23]. All the above-mentioned *KRR*-based one-class classifiers employ a single-layered architectures.

Over the last decade, stacked Auto-encoder based multi-layer architectures have received quite attention by researchers for multi-class or binary class classification tasks [24, 25]. Such architectures can lead to better representation learning [26, 27] and also used in dimensionality reduction [28, 29, 30]. High-level feature representations obtained by using stacked Auto-Encoder also helps in improving the performance of the traditional classifiers [31]. Moreover, this concept is also extended for kernel-based learning [32, 33]. Recently, Wong et al. [34] explores *KRR*-based representation learning for the multi-class classification task. Inspired by the advantage of multi-layer architecture, this paper explores the possibility of *KRR*-based representation learning for the one-class classification task.

In this paper, we propose a multi-layer architecture by stacking various *KRR*-based Auto-Encoder (trained using unsupervised learning) in a hierarchical manner for one-class classification task. After stacking several Auto-Encoder layers in a hierarchical manner, data are represented in a new feature space in which regression-based one-class classification is employed in the final layer. Overall architecture is referred as **Multi-layer KRR-based architecture for One-class Classification (MKOC)**. The multiple layers exploit the idea of successive nonlinear data mappings

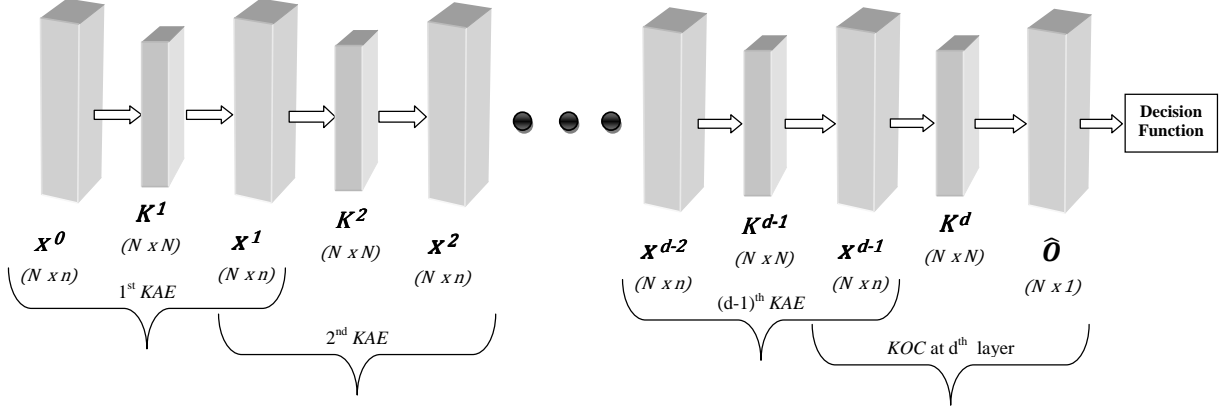


Figure 1: Schematic Diagram of *MKOC*

and hence capture the relationship effectively. During the training process of the Auto-Encoder, it simultaneously enhances the data reconstruction and data representation ability of the classifier. Output of the stacked Auto-Encoder is approximated to any real number and set a threshold for deciding whether any sample is outlier or not. Two types of threshold deciding criteria are discussed so far in this paper.

Further, the *MKOC* performance is evaluated using 15 benchmark datasets and its performance is compared with 11 state-of-the-art kernel-based methods available in the literature. Finally, a Friedman test [35] is conducted to verify the statistical significance of the experimental outcomes of *MKOC* classifier and it rejects the null hypothesis with 95% confidence level.

The rest of the paper is organized as follows. Section 2 describes the *MKOC* in detail. Performance evaluation is provided in Section 3. Finally, Section 4 concludes our work.

2. Multi-Layer KRR based Once-Class Classifier

In this section, a **Multi-layer KRR-based architecture for One-class Classification (*MKOC*)** is described. The proposed multi-layer architecture is constructed by stacking various *KRR*-based Auto-Encoders (*KAEs*), followed by a *KRR*-based one-class classifier (*KOC*), as shown in Fig. 1. These stacked Auto-Encoders are employed for defining the successive data representation. In the 1st *KAE* of this figure, input training matrix is denoted by $X = X^0 = \{x_i^0\}$, where $x_i^0 = [x_{i1}^0, x_{i2}^0, \dots, x_{in}^0]$, $i = 1, 2, \dots, N$, is the n -dimensional input vector of the i^{th} training sample. Let us assume that there are d layers in the proposed architecture, i.e., $h = 1, 2, \dots, d$. Output of the h^{th} layer is passed as input to the $(h + 1)^{\text{th}}$ layer. Let us denote output at h^{th} layer of Auto-Encoder, $X^h = \{x_i^h\}$, where $x_i^h = [x_{i1}^h, x_{i2}^h, \dots, x_{in}^h]$, $i = 1, 2, \dots, N$. X^h corresponds to the output of the h^{th} Auto-Encoder and the input of the $(h + 1)^{\text{th}}$ Auto-Encoder. Each

of the Auto-Encoders involves a data mapping using function $\phi(\cdot)$, mapping X^{h-1} to $\phi^h = \phi(X^{h-1})$. $\phi(\cdot)$ corresponds to a mapping of X^{h-1} to the corresponding kernel space $\mathbf{K}^h = (\Phi^h)^T \Phi^h$. Here, $\Phi^h = [\phi_1^h, \phi_2^h, \dots, \phi_N^h]$. The data representation obtained by calculating the output of the $(d-1)^{th}$ Auto-Encoder in the architecture is passed to the d^{th} layer for OCC using *KOC*. Two types of training errors are generated by *MKOC*. One is generated by the Auto-Encoder until $d-1$ layers and denoted as an error matrix $\mathbf{E}^h = \{e_i^h\}$, where $i = 1, 2, \dots, N$ and $h = 1, 2, \dots, (d-1)$. And other is generated by the one-class classifier at d^{th} layer which is denoted as an error vector $\mathbf{E}^d = \{e_i^d\}$, where $i = 1, 2, \dots, N$. The overall architecture of *MKOC* is formed by two processing steps.

In **first step**, $(d-1)$ *KAEs* are trained, each defining a pair (X^h, β_a^h) , and stacked in a hierarchical manner. Here, β_a^h denotes weight matrix of the h^{th} Auto-Encoder. A *KAE* minimizes the following criterion, which involves a non-linear² feature mapping $X^{h-1} \rightarrow \Phi^h$:

$$\text{Minimize : } \mathfrak{L}_{KAE} = \frac{1}{2} \|\beta_a^h\|^2 + \frac{C}{2} \sum_{i=1}^N \|e_i^h\|_2^2 \quad (1)$$

$$\text{Subject to : } (\beta_a^h)^T \phi_i^h = x_i^{h-1} - e_i^h, \quad i = 1, 2, \dots, N,$$

where C is a regularization parameter, and e_i^h is a training error vector corresponding to the i^{th} training sample at h^{th} layer. Based on the Representer Theorem [36], we express β_a^h as a linear combination of the training data representation Φ^h and a reconstruction weight matrix \mathbf{W}_a^h :

$$\beta_a^h = \Phi^h \mathbf{W}_a^h. \quad (2)$$

Hence, by using Representer Theorem [36], minimization criterion in (1) is reformulated as follows:

$$\text{Minimize : } \mathfrak{L}_{KAE} = \frac{1}{2} \text{Tr}((\mathbf{W}_a^h)^T (\Phi^h)^T \Phi^h \mathbf{W}_a^h) + \frac{C}{2} \sum_{i=1}^N \|e_i^h\|_2^2, \quad (3)$$

$$\text{Subject to : } (\mathbf{W}_a^h)^T (\phi_i^h)^T \phi_i^h = x_i^{h-1} - e_i^h, \quad i = 1, 2, \dots, N.$$

By further substitution of $\mathbf{K}^h = (\Phi^h)^T \Phi^h$, where $k_i^h \subseteq \mathbf{K}^h$ is formed by the elements $k_{ij}^h = (\phi_i^h)^T \phi_j^h$, the criterion in (3) can be written as:

$$\text{Minimize : } \mathfrak{L}_{KAE} = \frac{1}{2} \text{Tr}((\mathbf{W}_a^h)^T \mathbf{K}^h \mathbf{W}_a^h) + \frac{C}{2} \sum_{i=1}^N \|e_i^h\|_2^2, \quad (4)$$

$$\text{Subject to : } (\mathbf{W}_a^h)^T k_i^h = x_i^{h-1} - e_i^h, \quad i = 1, 2, \dots, N.$$

²Linear case can be easily derived from (1) by substituting $\phi_i^h \rightarrow x_i^{h-1}$

The Lagrangian relaxation of (4) is shown below in (5):

$$\begin{aligned} \mathfrak{L}_{KAE} = & \frac{1}{2} Tr((\mathbf{W}_a^h)^T \mathbf{K}^h \mathbf{W}_a^h) + \frac{C}{2} \sum_{i=1}^N \|\mathbf{e}_i^h\|_2^2 \\ & - \sum_{i=1}^N \alpha_i^h ((\mathbf{W}_a^h)^T \mathbf{k}_i^h - \mathbf{x}_i^{h-1} + \mathbf{e}_i^h) \end{aligned} \quad (5)$$

where $\alpha = \{\alpha_i^h\}$, $i = 1, 2 \dots N$, is a Lagrangian multiplier. In order to optimize \mathfrak{L}_{KAE} , we compute its derivatives as follows:

$$\frac{\partial \mathfrak{L}_{KAE}}{\partial \mathbf{W}_a^h} = 0 \Rightarrow \mathbf{W}_a^h = \alpha \quad (6)$$

$$\frac{\partial \mathfrak{L}_{KAE}}{\partial \mathbf{e}_i^h} = 0 \Rightarrow \mathbf{E}^h = \frac{1}{C} \alpha \quad (7)$$

$$\frac{\partial \mathfrak{L}_{KAE}}{\partial \alpha_i^h} = 0 \Rightarrow (\mathbf{W}_a^h)^T \mathbf{K}^h = \mathbf{X}^{h-1} - \mathbf{E}^h \quad (8)$$

The matrix \mathbf{W}_a^h is obtained by substituting (7) and (8) into (6), and is given by:

$$\mathbf{W}_a^h = \left(\mathbf{K}^h + \frac{\mathbf{I}}{C} \right)^{-1} (\mathbf{X}^{h-1})^T \quad (9)$$

Now, β_a^h can be derived by substituting (9) into (2):

$$\beta_a^h = \Phi^h \left(\mathbf{K}^h + \frac{\mathbf{I}}{C} \right)^{-1} (\mathbf{X}^{h-1})^T \quad (10)$$

Hence, the transformed data \mathbf{X}^h by the h^{th} KAE can be obtained as follows:

$$\mathbf{X}^h = (\Phi^h)^T \beta_a^h = (\Phi^h)^T \Phi^h \mathbf{W}_a^h = \mathbf{K}^h (\mathbf{W}_a^h)^T \quad (11)$$

where $\mathbf{K}^h \in \mathbb{R}^{N \times N}$ is the kernel matrix for the h^{th} layer. After mapping the training data through the $(d-1)$ successive KAEs **in the first step**, the training data representations defined by the outputs of the $(d-1)^{\text{th}}$ KAE are used in order to train a KOC **in the second step**. KOC involves a nonlinear feature mapping $\mathbf{X}^{d-1} \rightarrow \Phi^d$ and is trained by solving

the following optimization problem:

$$\begin{aligned} \text{Minimize : } \mathfrak{L}_{MKOC^d} &= \frac{1}{2} \|\beta_o^d\|^2 + \frac{C}{2} \sum_{i=1}^N \|e_i^d\|_2^2 \\ \text{Subject to : } (\beta_o^d)^T \phi_i^d &= r - e_i^d, \quad i = 1, 2, \dots, N \end{aligned} \quad (12)$$

where e_i^d is training error corresponding to i^{th} training sample and β_o^d denotes weight vector at d^{th} layer. By using Representer Theorem [36], β_o^d is expressed as a linear combination of the training data representation Φ^d and reconstruction **weight vector** W_o^d :

$$\beta_o^d = \Phi^d W_o^d. \quad (13)$$

Hence, the minimization criterion in (12) is reformulated to the following:

$$\begin{aligned} \text{Minimize : } \mathfrak{L}_{MKOC^d} &= \frac{1}{2} (W_o^d)^T (\Phi^d)^T \Phi^d W_o^d + \frac{C}{2} \sum_{i=1}^N \|e_i^d\|_2^2 \\ \text{Subject to : } (W_o^d)^T (\phi_i^d)^T \phi_i^d &= r - e_i^d, \quad i = 1, 2, \dots, N \end{aligned} \quad (14)$$

In addition, by substituting $K^d = (\Phi^d)^T \Phi^d$, where $k_i^d \subseteq K^d$, the optimization problem in (14) can be reformulated as follows:

$$\begin{aligned} \text{Minimize : } \mathfrak{L}_{MKOC^d} &= \frac{1}{2} (W_o^d)^T K^d W_o^d + \frac{C}{2} \sum_{i=1}^N \|e_i^d\|_2^2, \\ \text{Subject to : } (W_o^d)^T k_i^d &= r - e_i^d, \quad i = 1, 2, \dots, N. \end{aligned} \quad (15)$$

The Lagrangian relaxation of (15) is shown below in (16):

$$\begin{aligned} \mathfrak{L}_{MKOC^d} &= \frac{1}{2} (W_o^d)^T K^d W_o^d + \frac{C}{2} \sum_{i=1}^N \|e_i^d\|_2^2 \\ &\quad - \sum_{i=1}^N \alpha_i^d ((W_o^d)^T k_i^d - r + e_i^d) \end{aligned} \quad (16)$$

where $\alpha = \{\alpha_i^d\}, i = 1, 2, \dots, N$, is a Lagrangian multiplier. In order to optimize \mathfrak{L}_{MKOC^d} , we compute its derivatives as follows:

$$\frac{\partial \mathfrak{L}_{MKOC^d}}{\partial W_o^d} = 0 \Rightarrow W_o^d = \alpha \quad (17)$$

$$\frac{\partial \mathfrak{L}_{MKOC^d}}{\partial e_i^d} = 0 \Rightarrow E^d = \frac{1}{C} \alpha \quad (18)$$

$$\frac{\partial \mathcal{E}_{MKOC^d}}{\partial \alpha_i^d} = 0 \Rightarrow (\mathbf{W}_o^d)^T \mathbf{K}^d = \mathbf{r} - \mathbf{E}^d \quad (19)$$

The matrix \mathbf{W}_o^d of d^{th} layer is, thus, obtained by substituting (18) and (19) into (17), and is given by:

$$\mathbf{W}_o^d = \left(\mathbf{K}^d + \frac{\mathbf{I}}{C} \right)^{-1} \mathbf{r} \quad (20)$$

β_o^d can be derived by substituting (20) in (13):

$$\beta_o^d = \Phi^d \left(\mathbf{K}^d + \frac{\mathbf{I}}{C} \right)^{-1} \mathbf{r}, \quad (21)$$

where \mathbf{r} is a vector having all elements equal to r . Since the value r can be arbitrary, we set it equal to $r = 1$.

The predicted output of the final layer (i.e., d^{th} layer) of the multi-layer architecture for training samples can be calculated as follows:

$$\widehat{\mathbf{O}} = (\Phi^d)^T \beta_o^d = (\Phi^d)^T \Phi^d \mathbf{W}_o^d = \mathbf{K}^d (\mathbf{W}_o^d)^T \quad (22)$$

where $\widehat{\mathbf{O}}$ is the predicted output for training data.

After completing the training process, a threshold is required to decide whether any sample is an outlier or not which is discussed in the next subsection.

2.1. Decision Function

Two types of thresholds namely, θ_1 and θ_2 , are employed with the proposed method, which are determined as follows:

1. For θ_1 :

- (i) Calculate distance between the predicted value of the i^{th} training sample and r , and store in a vector \mathbf{d} as follows:

$$d(i) = \left| \widehat{O}_i - r \right| \quad (23)$$

- (ii) After storing all distances in \mathbf{d} as per (23), sort these distances in decreasing order and denoted by a vector \mathbf{d}_{dec} . Further, reject few percent of training samples based on the deviation. Most deviated samples are rejected first because they are most probably far from the distribution of the target data. The threshold is decided based on these deviations as follows:

$$\theta_1 = d_{dec}(\lfloor \eta * N \rfloor) \quad (24)$$

where $0 < \eta \leq 1$ is the fraction of rejection of training samples for deciding threshold value. N is the number of training samples and $\lfloor \cdot \rfloor$ denotes floor operation.

2. **For θ_2 :** Select threshold (θ_2) as a small fraction of the mean of the predicted output:

$$\theta_2 = (\lfloor \eta * \text{mean}(\widehat{O}) \rfloor) \quad (25)$$

where $0 < \eta \leq 1$ is the fraction of rejection for deciding threshold value.

Hence, a threshold value can be determined by above procedures. Afterwards, during testing, a test vector \mathbf{x}_p is fed to the trained multi-layer architecture and its output \widehat{O}_p is obtained. Further, compute \widehat{d} for both types of threshold as follows:

For θ_1 , calculate the distance (\widehat{d}) between the predicted value \widehat{O}_p of the p^{th} testing sample and r :

$$\widehat{d} = |\widehat{O}_p - r| \quad (26)$$

For θ_2 , calculate the distance (\widehat{d}) between the predicted value \widehat{O}_p of the p^{th} testing sample and mean of the predicted values obtained after training as follows:

$$\widehat{d} = |\widehat{O}_p - \text{mean}(\widehat{O})| \quad (27)$$

Algorithm 1 Multi-layer KRR-based architecture for OCC: *MKOC*

Input: Training set X , regularization parameter (C), kernel function (Φ), number of layers (d)

Output: Whether incoming sample is target or outlier

- 1: Initially, $X^0 = X$
 - 2: **for** $h = 1$ to d **do**
 - 3: **if** $h < d$ **then**
 - 4: **First Phase:** *KAEs* are stacked from first to $(d-1)^{\text{th}}$ layer in the hierarchical fashion and transform the input samples.
 - 5: Train the *KAE* as per Eq. (4).
 - 6: Transformed output X^h for the input X^{h-1} is computed to pass as the input to the next layer in the hierarchy.
 - 7: **else**
 - 8: **Second Phase:** Final layer, i.e., d^{th} layer for one-class classification.
 - 9: Output of $(d-1)^{\text{th}}$ Auto-Encoder is passed as an input to one-class classifier at d^{th} layer.
 - 10: Train the d^{th} layer by *MKOC^d* as per Eq. (15).
 - 11: **end if**
 - 12: **end for**
 - 13: Compute a threshold either θ_1 (Eq. (24)) or θ_2 (Eq. (25)).
 - 14: At final step, whether a new input is outlier or not, decides based on the rule discussed in Eq. (28).
-

Finally, x_p is classified based on the following rule:

$$\begin{aligned} &\text{If } \widehat{d} \leq \text{Threshold, } x_p \text{ belongs to normal class} \\ &\text{Otherwise, } x_p \text{ is an outlier} \end{aligned} \tag{28}$$

The overall processing steps followed by *MKOC* are described in Algorithm 1.

The above-described multi-layer OCC architecture creates two variants of *MKOC* using two types of threshold criteria (viz., θ_1 and θ_2), i.e., *MKOC_θ1* and *MKOC_θ2*.

3. Performance Evaluation

In this section, experiments are conducted to evaluate the performance of the proposed MKOC over 15 data sets. These datasets are obtained from University of California Irvine (UCI) repository [37] and were originally generated for the binary or multi-class classification task. For our experiments, we have made it compatible with OCC task in the following ways. If a dataset has two classes then, alternately, we use each of the classes in the binary dataset as the target class and the remaining one as outlier. If a dataset has more than two classes then we use one of the classes in the dataset as the target class and the remaining ones as outliers. In this way, we construct 15 one-class datasets from 8 multi-class datasets. Description of these datasets can be found in Table 1. These 15 datasets can be divided into 3 category viz., 6 financial, 6 medical and 3 miscellaneous datasets. Many of the datasets are slightly imbalanced. Class imbalance ratio of both of the classes are approximately 1 : 2 in case of 7 datasets viz., German(1), German(2), Pima(1), Pima(2), Glass(1), Glass(2), and Iris. All experiments on these datasets are carried out with MATLAB 2016a on Windows 7 (Intel Xeon 3 GHz processor, 64 GB RAM) environment.

Total 11 existing kernel-based one-class classifiers are employed for comparison purpose, which can be categorized as follows:

- (i) Support Vector Machine (*SVM*) based: **One-class SVM (OCSVM)** [13], **Support Vector Data Description (SVDD)** [12]
- (ii) *KRR*-based:
 - (a) Without Graph-Embedding: **KRR-based OCC (KOC)** [20] and **KRR-based Auto-Encoder model for OCC (AEKOC)** [21]
 - (b) With Graph-Embedding: Two types of Graph-Embedding, i.e., Local and Global, have been explored in the literature. **Local and Global Graph-Embedding with KOC** are named as *LKOC-X* [22] and *GKOC-X*

[22, 23], respectively. Here, X can be any Laplacian Graph with local or global Graph-embedding. For local, two types of Graphs are explored viz., **Local Linear Embedding (LLE)** and **Laplacian Eigenmaps (LE)**. For global, four types of Graphs are explored viz., **Linear Discriminant Analysis (LDA)**, **Clustering-based LDA (CDA)**, **class variance (CV)**, and **sub-class variance (SV)**. Hence, final six variants are generated namely, *LKOC-LE*[22], *LKOC-LLE* [22], *GKOC-LDA* [22], *GKOC-CDA*[22], *GKOC-CV*[23] and *GKOC-SV*[23].

(iii) Principal Component Analysis (PCA) based: **Kernel PCA (KPCA)**[14].

All one-class classifiers are implemented and tested in the same environment. *OC SVM* is implemented using LIBSVM library [38]. *SVDD* is implemented by using DD Toolbox [39].

Codes of all *KRR*-based one-class classifiers were provided by the authors of the corresponding papers. The implementations of *KPCA*[14] and *AEKOC*[21] are obtained from the links given in the paper (links are made available at the reference of the corresponding paper).

Table 1: Datasets Description

| S. No. | Name | #Targets | #Outliers | #Features | #samples |
|---|--------------|----------|-----------|-----------|----------|
| Financial Credit Approval Datasets | | | | | |
| 1 | German(1) | 700 | 300 | 24 | 1000 |
| 2 | German(2) | 300 | 700 | 24 | 1000 |
| 3 | Australia(1) | 307 | 383 | 14 | 690 |
| 4 | Australia(2) | 383 | 307 | 14 | 690 |
| 5 | Japan(1) | 294 | 357 | 15 | 651 |
| 6 | Japan(2) | 357 | 294 | 15 | 651 |
| Medical Disease Datasets | | | | | |
| 7 | Heart(1) | 160 | 137 | 13 | 297 |
| 8 | Heart(2) | 137 | 160 | 13 | 297 |
| 9 | Pima(1) | 500 | 268 | 8 | 768 |
| 10 | Pima(2) | 268 | 500 | 8 | 768 |
| 11 | Bupa(1) | 145 | 200 | 6 | 345 |
| 12 | Bupa(2) | 200 | 145 | 6 | 345 |
| Miscellaneous Datasets | | | | | |
| 13 | Glass(1) | 76 | 138 | 9 | 214 |
| 14 | Glass(2) | 138 | 76 | 9 | 214 |
| 15 | Iris | 50 | 100 | 4 | 150 |

For all of the kernel-based methods, Radial Basis Function (RBF) kernel is employed as shown below,

$$\kappa(x_i, x_j) = \exp\left(-\frac{\|x_i - x_j\|_2^2}{2\sigma^2}\right) \quad (29)$$

where σ is calculated as the mean Euclidean distance between training vectors in the corresponding feature space. For the proposed multi-layer architecture (*MKOC*), we have used maximum $d = 5$ layers and the value of σ^h is calculated at each h^{th} layer independently using the training data representations X^{h-1} . At each layer, regularization parameter is selected from the range of $\{2^{-3}, \dots, 2^3\}$. The classifiers which exploit graphs, i.e., *LKOC-X*, *GKOC-X*, and *GKOC-XX*, have two regularization parameters, which are selected based on the cross-validation using values 2^l , where $l = \{-3, \dots, 3\}$. For graph encoding subclass information in *GKOC-XX*, the number of subclasses is selected from the range $\{2, 3, \dots, 20\}$. For the *KOC* and *AEKOC* methods, regularization parameter is selected from the range $\{2^{-3}, \dots, 2^3\}$. For *KPCA* based OCC, the percentage of the preserved variance is selected from the range $[85, 90, 95]$. The fraction of rejection (η) of outliers during threshold selection is set equal to 0.05 for all methods.

3.1. Performance Evaluation Criteria

Geometric mean (η_g) is computed in the experiment for evaluating the performance of each of the classifiers and is calculated as

$$\eta_g = \sqrt{\text{Precision} * \text{Recall}} \quad (30)$$

In all our experiments, 5-fold cross-validation (CV) procedure is used and the average Gmean value (along with the corresponding standard deviation (Δ)) over 5-fold CV are reported in the results. η_g values of all the classifiers are further analyzed by using mean of all Gmeans (η_m) and percentage of the maximum Gmean (η_p). η_m is computed by taking average of all Gmeans obtained by a classifier over all datasets. η_p is computed as follows [40]:

$$\eta_p = \frac{\sum_{i=1}^{\text{no. of datasets}} \left(\frac{\text{Gmean of classifier for } i^{\text{th}} \text{ dataset}}{\text{Maximum Gmean achieved for } i^{\text{th}} \text{ dataset}} \times 100 \right)}{\text{Number of datasets}} \quad (31)$$

Moreover, Friedman testing is performed to verify the statistical significance of the obtained results. To this end, similar to [40], we also compute Friedman Rank (η_f)[35].

3.2. Performance Comparison

The Gmean (η_g) of the 13 kernel-based methods over 15 datasets are provided in Tables 2 to 4 for financial, medical, and miscellaneous datasets, respectively. Best η_g per dataset is displayed in boldface in these Tables. Out of 6 **financial** credit approval datasets, proposed multi-layer one-class classifier performs better for 4 datasets. In

Table 2: Performance in term of $\eta_g \pm \Delta$ (%) over 5-folds and 5 runs for financial datasets

| One-class Classifier | German(1) | German(2) | Australia(1) | Australia(2) | Japan(1) | Japan(2) |
|----------------------|------------------|-------------------|-------------------|-------------------|-------------------|-------------------|
| KPCA [14] | 80.77±0.07 | 49.75±0.28 | 63.69±0.29 | 73.06±0.18 | 64.09±0.29 | 72.29±0.29 |
| OCSVM [13] | 80.34±0.33 | 52.8±0.86 | 66.08±0.6 | 76.59±0.44 | 71.45±0.38 | 75.78±0.29 |
| SVDD [12] | 81.1±0.34 | 52.77±0.82 | 65.55±0.47 | 76.78±0.22 | 70.15±0.4 | 76.58±0.28 |
| KOC [20] | 73.17±0.26 | 53.41±0.3 | 65.07±0.68 | 74.21±1.12 | 67.33±1.24 | 73.48±1.62 |
| AEKOC [21] | 74.04±0.29 | 51.57±0.37 | 72.88±0.66 | 77.96±0.55 | 76.23±0.46 | 78.27±0.51 |
| GKOC-LDA [22] | 72.53±0.74 | 52.94±0.24 | 64.98±1.09 | 73.71±1.21 | 67.12±1.19 | 72.73±1.83 |
| LKOC-LE [22] | 72.75±0.5 | 53.06±0.34 | 65.09±0.82 | 74.03±1.26 | 67.24±1.2 | 73.15±1.63 |
| LKOC-LLE [22] | 70.86±0.52 | 52.51±0.7 | 62.95±0.64 | 70.72±0.68 | 64.97±0.39 | 69.79±1.52 |
| GKOC-CDA [22] | 72.6±0.66 | 52.9±0.15 | 67.48±1.67 | 73.74±1.2 | 74.58±2.56 | 72.75±1.8 |
| GKOC-CV[23] | 81.42±0.17 | 53.06±0.08 | 63.21±0.4 | 73.67±0.51 | 63.91±0.43 | 73.56±0.36 |
| GKOC-SV [23] | 79.39±1.63 | 53.49±0.39 | 63.9±0.67 | 74.6±1.16 | 66.17±0.69 | 73.96±0.92 |
| MKOC_θ1 | 74.1±0.86 | 54.46±0.11 | 72.12±0.76 | 79.89±0.75 | 74.45±0.59 | 80.14±0.76 |
| MKOC_θ2 | 82.79±0.3 | 49.59±0.76 | 72.43±0.52 | 80.31±0.45 | 74.66±0.83 | 80.55±0.28 |

Table 3: Performance in term of $\eta_g \pm \Delta$ (%) over 5-folds and 5 runs for medical datasets

| One-class Classifier | Heart(1) | Heart(2) | Pima(1) | Pima(2) | Bupa(1) | Bupa(2) |
|----------------------|-------------------|------------------|-----------------|------------------|------------------|------------------|
| KPCA [14] | 70.42±0.22 | 63.5±0.78 | 77.98±0.18 | 57.05±0.4 | 62.91±0.4 | 74.28±0.59 |
| OCSVM [13] | 72.91±0.55 | 64.9±1.4 | 79.18±0.19 | 56.59±0.47 | 60.64±1.3 | 69.78±0.19 |
| SVDD [12] | 72.91±0.55 | 64.9±1.4 | 79.21±0.19 | 56.71±0.62 | 60.64±1.23 | 69.75±0.21 |
| KOC [20] | 65.03±1.1 | 66.39±0.53 | 79.04±0.33 | 54.78±0.21 | 57.09±1.48 | 68.81±0.99 |
| AEKOC [21] | 67.99±0.94 | 61.15±0.68 | 78.66±0.28 | 54.01±0.39 | 56.19±0.68 | 68.31±0.53 |
| GKOC-LDA [22] | 64.44±0.92 | 62.88±0.8 | 78.94±0.47 | 54.57±0.3 | 57.04±1.37 | 68.81±1.04 |
| LKOC-LE [22] | 64.19±0.96 | 64.38±0.78 | 79.02±0.33 | 54.58±0.26 | 57.12±1.66 | 68.77±0.92 |
| LKOC-LLE [22] | 59±1.14 | 66±0.44 | 77.5±0.68 | 52.02±0.56 | 56.28±0.79 | 67.72±0.47 |
| GKOC-CDA [22] | 64.39±0.74 | 64.84±0.94 | 78.89±0.48 | 54.5±0.33 | 57.07±1.38 | 68.81±1.04 |
| GKOC-CV[23] | 69.02±0.67 | 65.66±0.4 | 77.56±0.14 | 58.91±0.4 | 62.78±0.56 | 74.42±0.9 |
| GKOC-SV [23] | 68.23±2.18 | 67.28±0.75 | 78.36±0.37 | 55.59±0.77 | 58.85±1.45 | 70.07±2.48 |
| MKOC_θ1 | 71.72±1.01 | 68.89±0.5 | 79.21±0.5 | 57.7±0.86 | 62.55±0.37 | 73.56±0.49 |
| MKOC_θ2 | 73.93±1.46 | 59.51±1.88 | 80.5±0.3 | 57.8±0.28 | 62.19±0.79 | 73.61±0.87 |

case of Australian(1) dataset, *MKOC_θ1* and *MKOC_θ2* yield significantly (>4%) better results compared to all of the methods presented in Table 2 except *AEKOC*. However, both exhibit comparable performance to *AEKOC*. Out of 6 **medical** datasets in Table 3, proposed multi-layer one-class classifier performs better for 3 datasets and yields comparable η_g for rest of the 3 datasets. Moreover, *MKOC_θ1* and *MKOC_θ2* perform better for 1 and 2 datasets, respectively. Further, among 3 **miscellaneous** datasets, *MKOC_θ1* yields better results for Glass(1) and Iris datasets.

Table 4: Performance in term of $\eta_g \pm \Delta$ (%) over 5-folds and 5 runs for three miscellaneous datasets

| One-class Classifier | Glass(1) | Glass(2) | Iris |
|----------------------|--------------------|-----------------|--------------------|
| KPCA [14] | 57.69±0.71 | 77.65±0.21 | 96.44±0.61 |
| OCSVM [13] | 59.61±0.55 | 73.32±0.88 | 85.06±2.6 |
| SVDD [12] | 59.61±0.55 | 72.89±0.69 | 84.12±2.86 |
| KOC [20] | 58.91±1.18 | 73.08±0.77 | 92.35±0.87 |
| AEKOC [21] | 59.29±1.03 | 73.22±0.77 | 92.79±0.91 |
| GKOC-LDA [22] | 58.55±1.73 | 73.14±0.56 | 89.67±0.63 |
| LKOC-LE [22] | 59.01±1.37 | 72.94±0.44 | 90.35±0.07 |
| LKOC-LLE [22] | 59.23±1.74 | 72.07±1.3 | 92.35±0.87 |
| GKOC-CDA [22] | 58.49±1.75 | 73.14±0.56 | 89.67±0.63 |
| GKOC-CV[23] | 56.7±1.41 | 79 ±1.54 | 94.69±1.01 |
| GKOC-SV [23] | 61.28±3.36 | 74.43±0.93 | 94.97±2.53 |
| MKOC_#1 | 62.46 ±1.51 | 77.15±0.47 | 99.59 ±0.56 |
| MKOC_#2 | 59.23±0.96 | 75.69±2.09 | 93.87±2.97 |

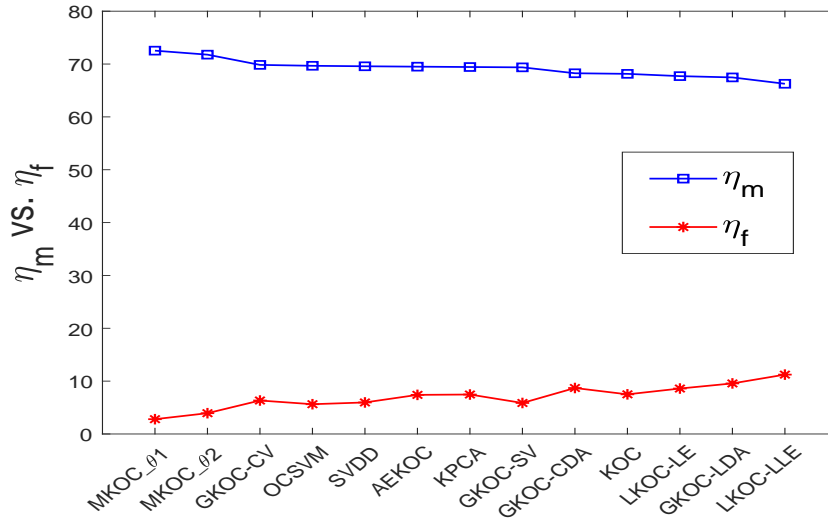


Figure 2: All one-class classifiers as per η_m in decreasing order and their corresponding Friedman Rank (η_f).

Table 5: η_f and η_m of all one-class classifiers in increasing order of the η_f (less value of η_f indicates better performance).

| One-class Classifier | η_f | $\eta_m(\%)$ |
|----------------------|----------|--------------|
| MKOC_01 | 2.80 | 72.53 |
| MKOC_02 | 3.93 | 71.78 |
| OCSVM | 5.63 | 69.67 |
| GKOC-SV | 5.87 | 69.37 |
| SVDD | 5.97 | 69.58 |
| GKOC-CV | 6.33 | 69.84 |
| AEKOC | 7.40 | 69.50 |
| KPCA | 7.47 | 69.44 |
| KOC | 7.50 | 68.14 |
| LKOC-LE | 8.60 | 67.71 |
| GKOC-CDA | 8.70 | 68.26 |
| GKOC-LDA | 9.57 | 67.47 |
| LKOC-LLE | 11.23 | 66.27 |

Especially, for Iris dataset, *MKOC_01* exhibits significant improvement ($>4\%$) of η_g compared to all of the methods presented in Table 4. In case of Glass(2) dataset, *MKOC_01* yields better result compared to all of the methods presented in Table 4 except *GKOC-CV* and *KPCA*. As we have discussed earlier that 7 datasets are imbalanced in nature, namely, German(1), German(2), Pima(1), Pima(2), Glass(1), Glass(2), and Iris. Out of these 7 datasets, proposed multi-layer one-class classifier performs better for 5 datasets. Moreover, *MKOC_01* and *MKOC_02* yield better results for 3 and 2 datasets, respectively.

Overall, it can be observed from the above discussion and Tables 2 to 4 that *MKOC_02*, *MKOC_01*, *GKOC-CV*, *AEKOC*, and *KPCA* yield best results for 5, 4, 3, 2 and 1 datasets, respectively. Further, we compute η_m and η_p for all the classifiers to analyze the η_g value more closely.

The performance of each method over the 15 datasets using the η_m metric is presented in Table 5 and is plotted in a decreasing order in Fig. 2. Based on the obtained results in Fig. 2, it can be clearly stated that both proposed variants of *MKOC*, i.e., *MKOC_01*, *MKOC_02* have achieved top two positions among 13 one-class classifiers as per η_m criterion. However, *GKOC-CV* yields best η_m among existing kernel-based one-class classifiers. It is to be noted that *MKOC_02* yields best η_g for maximum number (i.e., 5) of datasets, however, *MKOC_01* yields better η_m compared to *MKOC_02*. Hence, in order to further analyze the performance of the competing one-class classifiers, η_p is calculated as per Eq. (31), similar to [40].

η_p metric provides information regarding proximateness of each classifier towards maximum η_g value. As it can be seen in Table 6, *MKOC_01* and *MKOC_02* hold the top two positions similar to the ranking based on the η_m values in Fig. 2. In Fig. 3, η_p values of all 13 one-class classifiers are plotted in an increasing order for all of the datasets. *MKOC_01* is a multi-layer version of the single-layered classifier *KOC*. The plotted lines for these two classifiers

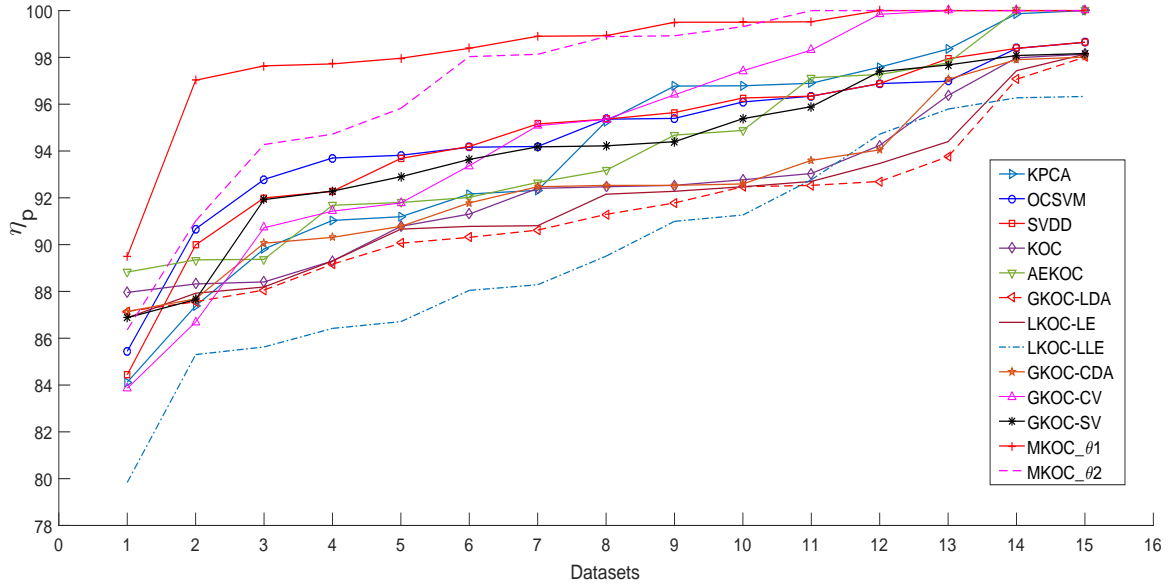


Figure 3: η_p achieved by various one-class classifiers over 15 datasets (ordered by increasing percentage)

Table 6: η_p value over 15 datasets

| One-class Classifiers | η_p (%) |
|-----------------------|--------------|
| MKOC_θ1 | 98.31 |
| MKOC_θ2 | 97.03 |
| GKOC-CV | 94.68 |
| OCSVM | 94.59 |
| SVDD | 94.48 |
| GKOC-SV | 94.04 |
| AEKOC | 94.04 |
| KPCA | 93.97 |
| GKOC-CDA | 92.57 |
| KOC | 92.40 |
| LKOC-LE | 91.84 |
| GKOC-LDA | 91.50 |
| LKOC-LLE | 89.86 |

in Fig. 3 clearly indicate the performance improvement of multi-layer version over single-layer one. Overall, Fig. 3 illustrates the clear superiority of the multi-layer one-class classifiers over the existing methods. Moreover, $MKOC_01$ obtains more than 97% η_p value for all datasets except German(1) dataset. Detailed η_p values for all 13 classifiers over 15 datasets are made available on the web page (<https://goo.gl/XLBtqp>).

Above discussion suggests $MKOC_01$ and $MKOC_02$ as the best performing classifier in term of η_g , η_m , and η_p . Despite this fact, a statistical testing needs to perform for verifying this fact. In the next subsection, Friedman Rank (η_f) testing is performed for statistical testing.

3.3. Statistical Comparison

For comparing the performance of the proposed variants $MKOC_01$ and $MKOC_02$ with the 11 existing kernel-based methods on 15 benchmark datasets, a non-parametric Friedman test is employed. In the Friedman test, the null hypothesis states that the mean of individual experimental treatment is not significantly different from the aggregate mean across all treatments and the alternate hypothesis states the other way around. Friedman test mainly computes three components viz., F-score, p-value and Friedman Rank (η_f). If the computed F-score is greater than the critical value at the tolerance level $\alpha = 0.05$, then one rejects the equality of mean hypothesis (i.e. null hypothesis). We employ the modified Friedman test [35] for the testing, which was proposed by Iman and Davenport [41]. The F-score obtained after employing non-parametric Friedman test is 7.28, which is greater than the critical value at the tolerance level $\alpha = 0.05$ i.e. $7.28 > 1.81$. Hence, null hypothesis can be rejected with 95% of a confidence level. The computed p-value of the Friedman test is $1.1461e - 08$ with the tolerance value $\alpha = 0.05$, which is much lower than 0.05. This small value indicates that differences in the performance of the various methods are statistically significant.

Afterwards, η_f of each classifier is also calculated to assign a rank to all 13 one-class classifiers. Friedman test assigns a rank to all the methods for each dataset, it assigns rank 1 to the best performing algorithm, the second best rank 2 and so on. If rank ties then average ranks are assigned [35]. The η_f value of all classifiers is provided in increasing order of its value (less value of η_f indicates better performance) in Table 5. These values are visualized in Fig. 2 with the decreasing order of η_m . $MKOC_01$ and $MKOC_02$ still achieve top two positions, similar to using the η_m metric. From Table 5 and Fig. 2, it can be observed that η_f of most of the classifiers follows a similar pattern as η_m , i.e., η_f increases as η_m decreases. However, some of the one-class classifiers don't follow the same pattern as with η_m like $GKOC-CV$ which has better η_m but inferior η_f compared to $OCSVM$ and $GKOC-SV$. The above analysis indicates that an one-class classifier with better η_f has better generalization capability compared to the other existing methods.

Overall, after the performance analysis of all the 13 one-class classifiers, it is observed that none of the existing one-class classifiers perform better than the proposed multi-layer one-class classifier in term various above discussed

performance criteria.

4. Conclusion

This paper has presented two variants of *KRR*-based multi-layer one-class classifier. It is constructed by stacking various Auto-Encoders followed by a *KRR*-based one-class classifier. Hence, two types of training processes are involved i.e. one is for *KAE* and other is for *KOC*. Extensive experimental comparisons have been provided with 11 state-of-the-art kernel feature mapping based one-class classifiers over 15 publicly available datasets in term of η_g , η_m , η_p , and η_f . These experiments have exhibited that the proposed multi-layer one-class classifier provides state-of-the-art performance. Stacked Auto-Encoder through multiple layers helps *MKOC* in achieving better generalization and data representation capability. Moreover, the statistical significance of the results has been verified by Friedman Ranking test. In future work, various other types of available Auto-Encoder can be explored to enhance the performance of the proposed multi-layer architecture.

Acknowledgment

This research was supported by Department of Electronics and Information Technology (DeITY, Govt. of India) under Visvesvaraya PhD scheme for electronics & IT.

References

- [1] M. A. Pimentel, D. A. Clifton, L. Clifton, and L. Tarassenko. A review of novelty detection. *Signal Processing*, 99:215–249, 2014.
- [2] C. Bellinger, S. Sharma, and N. Japkowicz. One-class classification - from theory to practice: A case-study in radioactive threat detection. *Expert Systems with Applications*, 2018.
- [3] H.-g. Bu, J. Wang, and X.-b. Huang. Fabric defect detection based on multiple fractal features and support vector data description. *Engineering Applications of Artificial Intelligence*, 22(2):224–235, 2009.
- [4] S. Zgarni, H. Keskes, and A. Braham. Nested svdd in dag svm for induction motor condition monitoring. *Engineering Applications of Artificial Intelligence*, 71:210–215, 2018.
- [5] D. M. J. Tax. One-class classification; concept-learning in the absence of counter-examples. *ASCI dissertation series*, 65, 2001.
- [6] B. Krawczyk and P. Filipczuk. Cytological image analysis with firefly nuclei detection and hybrid one-class classification decomposition. *Engineering Applications of Artificial Intelligence*, 31:126–135, 2014.
- [7] D. Li, S. Liu, and H. Zhang. A boundary-fixed negative selection algorithm with online adaptive learning under small samples for anomaly detection. *Engineering Applications of Artificial Intelligence*, 50:93–105, 2016.
- [8] A. De Paola, S. Gaglio, G. L. Re, F. Milazzo, and M. Ortolani. Adaptive distributed outlier detection for wsns. *IEEE Transactions on Cybernetics*, 45(5):902–913, 2015.
- [9] Liangwei Zhang, Jing Lin, and Ramin Karim. Sliding window-based fault detection from high-dimensional data streams. *IEEE Transactions on Systems, Man, and Cybernetics: Systems*, 47(2):289–303, 2017.

- [10] H.-P. Kriegel, A. Zimek, et al. Angle-based outlier detection in high-dimensional data. In *Proceedings of the 14th ACM SIGKDD international conference on Knowledge discovery and data mining*, pages 444–452. ACM, 2008.
- [11] N. Japkowicz. *Concept-learning in the absence of counter-examples: An autoassociation-based approach to classification*. PhD thesis, Rutgers, The State University of New Jersey, 1999.
- [12] D. M. J. Tax and R. P. W. Duin. Support vector domain description. *Pattern recognition letters*, 20(11):1191–1199, 1999.
- [13] B. Schölkopf, R. C. Williamson, A. J. Smola, J. Shawe-Taylor, and J. C. Platt. Support vector method for novelty detection. In *NIPS*, volume 12, pages 582–588, 1999.
- [14] H. Hoffmann. Kernel PCA for novelty detection. *Pattern Recognition*, 40(3):863–874, 2007. Software available at <http://www.heikohoffmann.de/kpca.html>.
- [15] C. Saunders, A. Gammerman, and V. Vovk. Ridge regression learning algorithm in dual variables. In *Proceedings of the Fifteenth International Conference on Machine Learning, ICML '98*, pages 515–521, San Francisco, CA, USA, 1998. Morgan Kaufmann Publishers Inc.
- [16] A. Verikas and M. Bacauskiene. Estimating ink density from colour camera rgb values by the local kernel ridge regression. *Engineering Applications of Artificial Intelligence*, 21(1):35–42, 2008.
- [17] M. Maalouf and D. Homouz. Kernel ridge regression using truncated newton method. *Knowledge-Based Systems*, 71:339–344, 2014.
- [18] S. Zhang, Q. Hu, Z. Xie, and J. Mi. Kernel ridge regression for general noise model with its application. *Neurocomputing*, 149:836–846, 2015.
- [19] X. Zhang, W. Chao, Z. Li, C. Liu, and R. Li. Multi-modal kernel ridge regression for social image classification. *Applied Soft Computing*, 67:117–125, 2018.
- [20] Q. Leng, H. Qi, J. Miao, W. Zhu, and G. Su. One-class classification with extreme learning machine. *Mathematical Problems in Engineering*, pages 1–11, 2014.
- [21] C. Gautam, A. Tiwari, and Q. Leng. On the construction of extreme learning machine for online and offline one-class classificationan expanded toolbox. *Neurocomputing*, 2017. Software available at <https://github.com/Chandan-IITI/One-Class-Kernel-ELM>.
- [22] A. Iosifidis, V. Mygdalis, A. Tefas, and I. Pitas. One-class classification based on extreme learning and geometric class information. *Neural Processing Letters*, pages 1–16, 2016.
- [23] V. Mygdalis, A. Iosifidis, A. Tefas, and I. Pitas. One class classification applied in facial image analysis. In *Image Processing (ICIP), 2016 IEEE International Conference on*, pages 1644–1648. IEEE, 2016.
- [24] Y. Bengio et al. Learning deep architectures for ai. *Foundations and trends® in Machine Learning*, 2(1):1–127, 2009.
- [25] J. Schmidhuber. Deep learning in neural networks: An overview. *Neural networks*, 61:85–117, 2015.
- [26] P. Vincent, H. Larochelle, Y. Bengio, and P.-A. Manzagol. Extracting and composing robust features with denoising autoencoders. In *Proceedings of the 25th international conference on Machine learning*, pages 1096–1103. ACM, 2008.
- [27] H.-C. Shin, M. R. Orton, D. J. Collins, S. J. Doran, and M. O. Leach. Stacked autoencoders for unsupervised feature learning and multiple organ detection in a pilot study using 4d patient data. *IEEE transactions on pattern analysis and machine intelligence*, 35(8):1930–1943, 2013.
- [28] G. E. Hinton and R. R. Salakhutdinov. Reducing the dimensionality of data with neural networks. *science*, 313(5786):504–507, 2006.
- [29] L. Van Der Maaten, E. Postma, and J. Van den Herik. Dimensionality reduction: a comparative. *J Mach Learn Res*, 10:66–71, 2009.
- [30] W. Wang, Y. Huang, Y. Wang, and L. Wang. Generalized autoencoder: A neural network framework for dimensionality reduction. In *Proceedings of the IEEE Conference on Computer Vision and Pattern Recognition Workshops*, pages 490–497, 2014.
- [31] P. Vincent, H. Larochelle, I. Lajoie, Y. Bengio, and P.-A. Manzagol. Stacked denoising autoencoders: Learning useful representations in a

- deep network with a local denoising criterion. *Journal of Machine Learning Research*, 11(Dec):3371–3408, 2010.
- [32] A. G. Wilson, Z. Hu, R. Salakhutdinov, and E. P. Xing. Deep kernel learning. In *Artificial Intelligence and Statistics*, pages 370–378, 2016.
- [33] C. Jose, P. Goyal, P. Aggrwal, and M. Varma. Local deep kernel learning for efficient non-linear svm prediction. In *International Conference on Machine Learning*, pages 486–494, 2013.
- [34] C. M. Wong, C. M. Vong, P. K. Wong, and J. Cao. Kernel-based multilayer extreme learning machines for representation learning. *IEEE Transactions on Neural Networks and Learning Systems*, 29(3):757–762, 2018.
- [35] J. Demšar. Statistical comparisons of classifiers over multiple data sets. *Journal of Machine learning research*, 7(Jan):1–30, 2006.
- [36] A. Argyriou, C. A. Micchelli, and M. Pontil. When is there a representer theorem? vector versus matrix regularizers. *Journal of Machine Learning Research*, 10(Nov):2507–2529, 2009.
- [37] M. Lichman. UCI machine learning repository, 2013.
- [38] C.-C. Chang and C.-J. Lin. LIBSVM: A library for support vector machines. *ACM Transactions on Intelligent Systems and Technology*, 2:27:1–27:27, 2011. Software available at <http://www.csie.ntu.edu.tw/~cjlin/libsvm>.
- [39] D. M. J. Tax. DDtools, the data description toolbox for MATLAB, version 2.1.2, June 2015.
- [40] M. Fernández-Delgado, E. Cernadas, S. Barro, and D. Amorim. Do we need hundreds of classifiers to solve real world classification problems. *J. Mach. Learn. Res*, 15(1):3133–3181, 2014.
- [41] R. L. Iman and J. M. Davenport. Approximations of the critical region of the fbietkan statistic. *Communications in Statistics-Theory and Methods*, 9(6):571–595, 1980.